Spatial and temporal distribution pattern of camptothecin in seeds and fruits of *Pyrenacantha volubilis* Hook. (Icacinaceae) during different fruit developmental stages

Hirenallur Kumarappa Suma[1,2], Vadlapudi Kumar[2], Patel Mohana Kumara[3], Amitava Srimany[3], Gudasalamani Ravikanth[1,5], Senthil Kumar Umapathy[1], Thalappil Pradeep[3], Ramesh Vasudeva[4] and Ramanan Uma Shaanker[1,*]

[1]School of Ecology and Conservation, and Department of Crop Physiology, University of Agricultural Sciences, GKVK, Bengaluru 560 065, India
[2]Department of Biochemistry, Davangere University, Shivagangothri, Davangere 577 002, India
[3]DST Unit of Nanoscience and Thematic Unit of Excellence, Department of Chemistry, Indian Institute of Technology Madras, Chennai 600 036, India
[4]Department of Forest Biology, College of Forestry, Sirsi 581 401, India
[5]Ashoka Trust for Research in Ecology and the Environment, Royal Enclave, Sriramapura, Jakkur, Bengaluru 560 064, India

Camptothecin (CPT), a quinoline indole alkaloid, is one of the important inhibitors of eukaryotic DNA topoisomerase I. The highest concentration of this alkaloid has been reported from the fruits of *Pyrenacantha volubilis* Hook. Here we report the spatial and temporal distribution pattern of CPT in seeds and fruits of *P. volubilis*. Temporally, CPT content was highest in mature but unripe fruits compared to ripened fruits. Spatially, cotyledonary tissues of the seed had the highest amount of CPT followed by seed coat and fruit coat. This pattern is best explained by selection to deter fruit predators during fruit development, but attracting the fruit dispersers when fruits are mature and ripe.

Keywords: Camptothecin, distribution pattern, fruit developmental stages, *Pyrenacantha volubilis*.

CAMPTOTHECIN (CPT), a quinoline indole alkaloid, is one of the important inhibitors of eukaryotic DNA topoisomerase I (ref. 1). Due to this property, two semi-synthetic analogues of CPT, namely topotecan and irinotecan (CPT-11) are used clinically against colon and ovarian cancers[2]. Camptothecin and its analogues have also been demonstrated to have anti-viral[3,4] and anti-parasitic activity[5].

Camptothecin has been reported from several species of families Apocynaceae, Loganiaceae, Icacinaceae, Rubiaceae and Nyssaceae, all belonging to the order Lamiids[6]. Recently, Suma *et al.*[7] reported the accumulation of CPT from fruits of *Pyrenacantha volubilis* Hook. (Icacinaceae), a climbing plant found on the eastern coast of India. This is by far the richest source of CPT reported so far. Besides CPT, the fruits also produce 9-methoxycamptothecin.

In the present study, the spatial and temporal pattern of CPT accumulation in the seeds and fruits of *P. volubilis* has been quantified by HPLC-PDA analysis. Derivatives and precursors of CPT were identified by their molecular mass using UFLC-ESI-MS. Using desorption electrospray ionization mass spectrometry imaging (DESI-MSI), the spatial distribution of CPT in seeds of *P. volubilis* during different fruit developmental stages was mapped. DESI-MSI technique is rapid and offers a spatially explicit resolution of the compounds present over a tissue surface. In recent years, MSI has been extensively used for studying the spatial distribution of secondary metabolites in flower petals of *Catharanthus roseus* L.[8], seeds of *Myristica malabarica* Lam.[9], fruits of *Dysoxylum binectariferum* Hook.f.ex Bedd.[10], seeds of *Hordeum vulgare* L.[11] and capsules of *Papaver somniferum* L.[12].

Pyrenacantha volubilis is a small climbing plant, ranging in height from a few feet to several metres. The plants occur in the dry scrub and deciduous forests of the eastern coast of southern India. They flower during August to September and bear small single-seeded fruits. The fruits ripen between December and February.

The taxonomic identity of the plant was established by one of the authors (S.K.U.), University of Agricultural Sciences at Bengaluru. The voucher specimens along with GPS coordinates, name of the site and date of collection are deposited at the School of Ecology and Conservation, University of Agricultural Sciences, Benglauru. Fruits of *P. volubili*s were collected from Mangalam sacred groves (79°44′22.2″E and 11°54′10.4″N) located on the eastern coast of Tamil Nadu, India. Six individuals were marked in Mangalam and the fruits were collected at different time intervals after anthesis. Size and weight of the fruits ranged from 14 to 16 mm (length), 8 to 11 mm (width) and 0.7 to 1.1 g. To track the time taken for fruit development, flowers on a few plants were date-tagged and followed through their development until final fruit set. Based on these observations, the fruits were sampled at the following time intervals for analysis: stage 1, immature (M1, 20 days after anthesis; bud formation stage); stage 2, semi-mature (M2, 35 days after anthesis; fruit expansion stage); stage 3, matured but green (M3, 50 days after anthesis; fruit maturation stage); stage 4, ripened (M4, 55 days after anthesis; ripening stage), and stage 5, overripened (M5, 70 days after anthesis; senescence stage; Figure 1 *a*).

Fruits corresponding to the five stages (M1 through M5) were collected from six randomly selected plants. Approximately 6–10 fruits per stage were collected from each of the plants. Fruits of the respective stages were

*For correspondence. (e-mail: umashaanker@gmail.com)

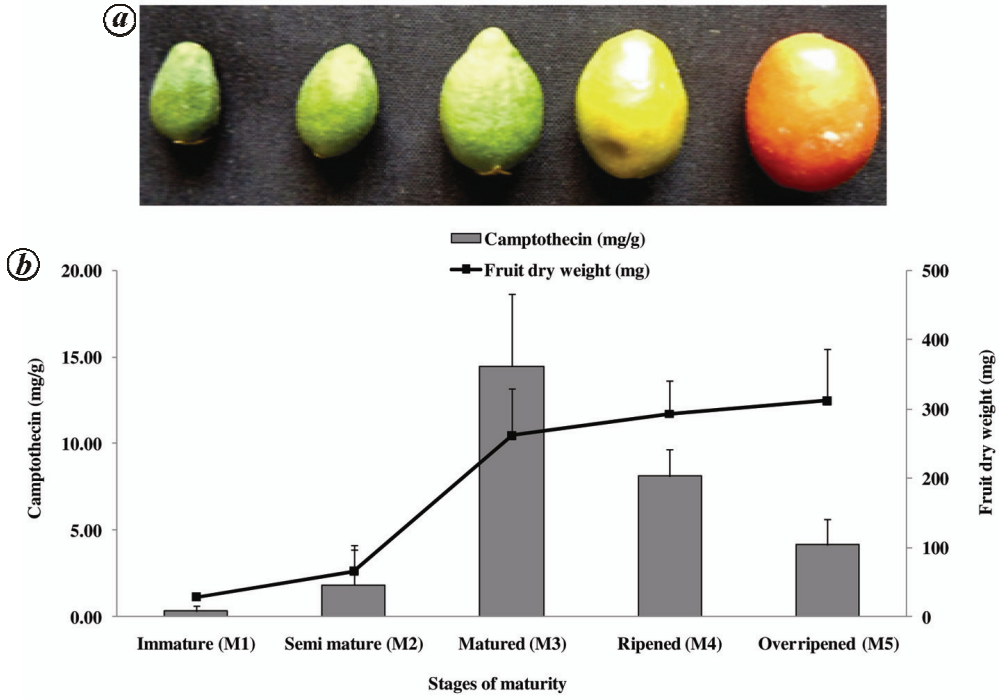

Figure 1. ***a***, Different stages of *Pyrenacantha volubilis* fruit (left to right M1 to M5). ***b***, Histogram showing camptothecin (mg/g dry wt of fruit) content in fruits at different developmental stages. Line indicates dry weight of the fruit (mg). Line over bars indicate standard deviation.

bulked (M1: $n = 45$, M2: $n = 50$, M3: $n = 60$, M4: $n = 50$ and M5: $n = 40$) and transferred into paper bags and dried in an hot-air oven at 50°C for 8 days. For temporal pattern analysis, CPT and related compounds were analysed for a random collection of the bulked fruits within each respective maturity stage (M1: $n = 10$, M2: $n = 10$, M3: $n = 10$, M4: $n = 10$ and M5: $n = 8$). For analysing CPT in the fruit parts, a random collection of dried fruits from stages M3 to M5 (M3: $n = 15$, M4: $n = 15$ and M5: $n = 15$) was separated into their constituent parts (fruit coat, seed coat and cotyledons). Fruits of stages M1 and M2 could not be separated into their constituent parts.

The obtained plant samples were ground to fine powder in pestle and mortar, and each sample was extracted in 5 ml of 61% ethanol at 60°C for 3 h in a water bath[6,13]. Then, 1 ml of the extract from each sample was centrifuged at 10,000 rpm (Mini Spin Plus, Eppendorf) for 10 min at room temperature. The supernatant was filtered using a 0.2 µm filter (Tarsons, India), and CPT and other related compounds were estimated using HPLC-PDA and UFLC-ESI-MS.

Camptothecin was quantified by HPLC-PDA (LC-20AD, Shimadzu, Japan). The conditions for the analysis were – column: RP-C18, 250 × 4.6 mm, 5 µm size (Phenomenex); detector: SPD-M 20A photodiode array detector (PDA), wavelength: 254 nm; flow rate: 1.5 ml/min; injection volume: 20 µl, mobile phase: pump A – 25% acetonitrile and pump B – 75% water + 0.1% trifluroacetic acid in an isocratic mode. By applying all these conditions the calibration curve was developed for CPT.

The CPT standard (Sigma Chemicals; 95% pure, HPLC-grade) was prepared using dimethyl sulphoxide (DMSO) and methanol in 1 : 3 (v/v) ratio at a concentration of 1 mg/ml. From the stock solution (1 mg/ml), working solution was prepared in the concentration range 0.100, 0.250, 0.500, 0.750 and 1.0 mg/ml respectively. Next, 20 µl working solution from each concentration was injected into the HPLC system. Calibration curve was constructed for each concentration against their peak area to obtain a regression curve ($y = 6E + 07x$; $R^2 = 0.998$). CPT in the samples was estimated based on the regression curve (Figure S1, see Supplementary Information online).

Camptothecin and related compounds present in the samples were analysed using UFLC-ESI-MS by subjecting the sample in a full scan positive ionization mode (LCMS-2020, Shimadzu, Japan). LC analysis was coupled to electrospray ionization mass spectrometry. LC conditions for the analysis were as follows: column – RPC-C18; 250 × 4.6 mm, 5 µm size (Phenomenex); detector – UV-Visible; wave length – 254 nm; flow rate – 0.5 ml/min; injection volume – 5 µl; mobile phase – pump A, 25% acetonitrile and pump B, 75% water in an isocratic mode. The total run time was 50 min. The conditions for mass spectrometric analysis were as follows: dry gas flow rate, 10 l/min; nebulizer gas pressure, 35 psi; nebulizing gas flow, 1.5 l/min, desolvation

temperature 250°C, and mass range 100–700 *m/z* with a single quadrupole mass analyser.

For DESI-MS imaging, fresh fruits corresponding to different fruit maturity stages were collected from the six plants described earlier. Seeds were manually removed from the fruits and washed thoroughly. Using a razor blade, cross-section of the seed was made roughly at its centre. The sections were impressed for 10–15 sec on a hot TLC plate kept on a heating mantle (~70°C) to get an imprint of the chemicals present in the seeds[14]. The TLC imprints were imaged by ambient DESI-MS. The imaging experiments were carried out using a mass spectrometer (Thermo Scientific LTQ XL) coupled with a 2D DESI ion source (Prosolia Inc.). A 7:3 v/v mixture of acetonitrile and water was used as solvent[15], and sprayed with a flow rate of 5 µl/min at an angle of 60° to the surface and 150 psi nebulizer gas (nitrogen) pressure. The following parameters were used for DESI-MS experiments: source voltage, 5 kV; capillary temperature, 250°C; capillary voltage, 45 V; and tube lens voltage, 100 V. Data were acquired in positive ion mode, and FireFly software was used to process the Xcalibur Raw Files as well as to create the image files (IMG File). BioMAP software was used for viewing the images. Fragmentation was done using collision-induced dissociation.

Temporally, CPT accumulation was maximum at mature green stage of fruits (M3: 14.48 mg/g dry wt), compared to immature (M1: 0.34 mg/g dry wt) and semi-mature (M2: 1.86 mg/g dry wt) fruits. In contrast, there was a significant reduction of CPT in ripened (M4: 8.14 mg/g dry wt) and overripened (M5: 4.17 mg/g dry wt) fruits (Figure 1). Single factor analysis of variance (ANOVA) indicated significant differences in mean CPT content in fruits across different developmental stages ($P < 0.001$). Spatially, CPT content was maximum in the cotyledonary tissue of mature green fruits (M3: 25.52 mg/g dry wt) compared to seed coat (M3: 3.36 mg/g dry wt) and fruit coat (M3: 2.10 mg/g dry wt; Figure 2).

Besides CPT *m/z* 349, the fruits also contained several other derivatives such as 10-hydroxycamptothecin *m/z* 365, 9-methoxycamptothecin *m/z* 379, 20-deoxycamptothecin *m/z* 333 and CPT precursors such as strictosamide *m/z* 499 and deoxypumiloside *m/z* 497 (Figure 3 and Figure S2 (see Supplementary Information online)). Across the fruit developmental stages, the relative magnitude of strictosamide *m/z* 499 and deoxyplumoside *m/z* 497 was highest at stage M4; at this stage, the CPT content had begun to decline. In contrast to stage M3 fruits, which had the highest CPT content, there was a decline in the relative magnitude of strictosamide and deoxypumiloside compared to stage M4 fruits.

The decline in CPT content over the seed developmental stages was also deciphered by DESI-MSI. Full mass spectrum analysis failed to reveal clear signature of CPT *m/z* 349 due to poor signal-to-noise ratio. However, a MS^2 spectrum of *m/z* 349 yielded the clear signature of the daughter ion at *m/z* 305, corresponding to the fragmentation ion of CPT (Figure 4 and Figure S3 (see Supplementary Information online)). The *m/z* 305 signal was most prominent in stage M3 and stage M4 seeds, while being significantly lower in stage M2 and stage M5 seeds. Within the cotyledon itself, CPT distribution was nearly uniform.

In summary, the results of this study indicate a temporal and spatial pattern of CPT accumulation in developing seeds and fruits of *P. volubilis*. Temporally, CPT accumulation was maximum at stage M3 of fruit development, corresponding to the mature green stage of fruits. Spatially, cotyledonary tissues of the seed had the highest amount of CPT followed by seed coat and fruit coat. Within the cotyledon, the distribution of CPT as evident from DESI-MSI, was nearly uniform. These results confirm the general patterns reported earlier for several secondary metabolites during seed development[16]. Several studies have also reported that secondary metabolites accumulate in developing seeds, presumably to confer resistance against abiotic and biotic stress during seed dispersal and germination[17]. These secondary metabolites may be either synthesized *de novo* in the seeds from available precursors[18], or transported from their sites of synthesis elsewhere in the plant[16,18].

The distinctive temporal pattern, where mature green fruits tend to show higher CPT content than stages before or after, has been reported for several secondary metabolites as well. For instance, in several solanaceous plants such as *Solanum mammosum* L.[19] and *Solanum khasianum* Clarke[20] the pattern of distribution of steroidal alkaloids follows that of CPT in *P. volubilis*, with early and ripened stages having less steroidal compound compared to mature green stage of the fruit. In *Lycopersicon esculentum* Mill., steroidal glycoalkaloids, α-tomatine decreased with ripening and the level of lycopene increased dramatically during ripening[21]. Hebbar *et al.*[22] reported

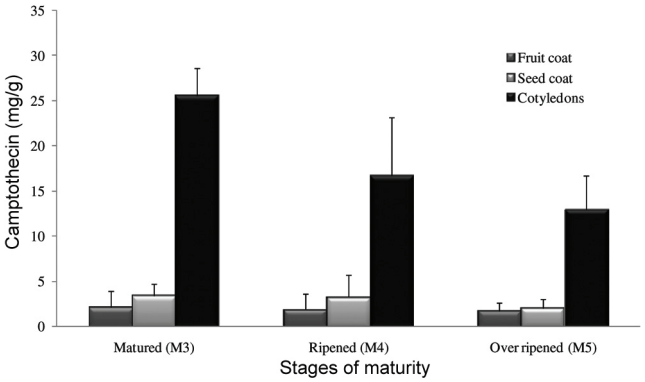

Figure 2. Camptothecin (mg/g) in different parts of *P. volubilis* fruit across the maturity stages. Line over bars indicate standard deviation.

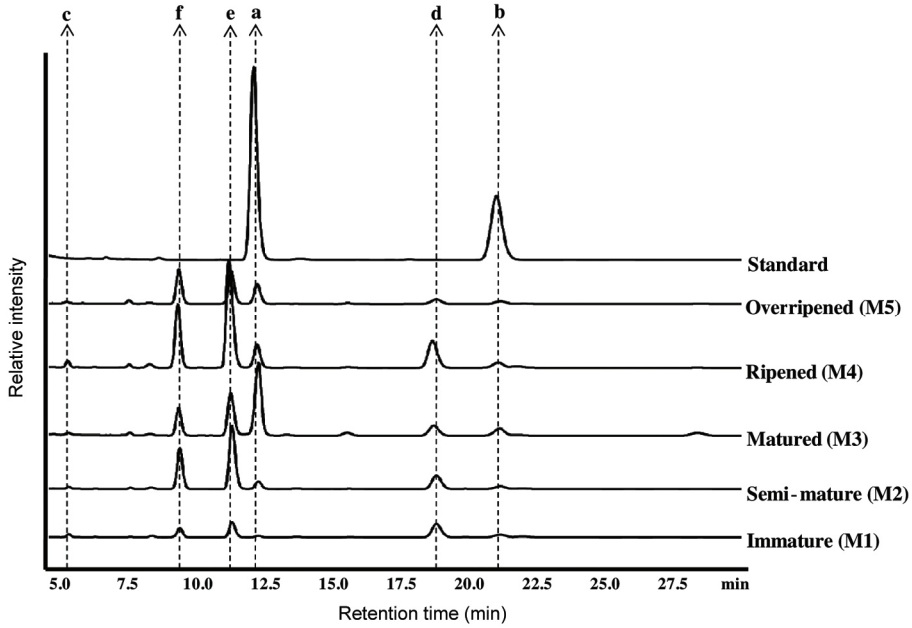

Figure 3. Liquid chromatography profile of *P. volubilis* fruit extracts from different fruit developmental stages – (a) camptothecin, (b) 9-methoxycamptothecin, (c) 10-hydroxycamptothecin, (d) strictosamide, (e) deoxypumiloside and (f) unknown compound.

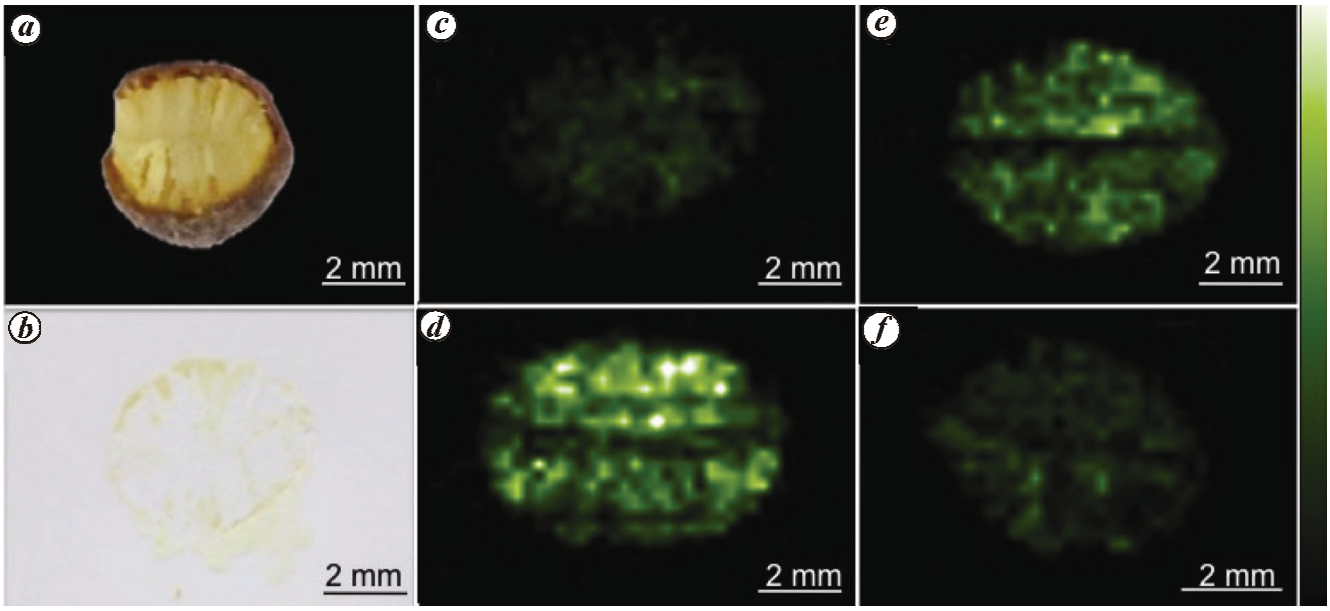

Figure 4. DESI-MS images of *m/z* 305, fragment ion of *m/z* 349 from *P. volubilis* during different developmental stages of the fruits. ***a***, Cross-section of *P. volubilis* seed; ***b***, TLC imprint of seed; ***c***, Semi-mature: M2; ***d***, Matured: M3; ***e***, ripened: M4; ***f***, Overripened: M5.

that trypsin proteinase inhibitors tend to accumulate most in mature green fruits and were significantly less in immature and fully ripened fruits. The authors argue that the observed pattern was probably to deter predators during the immature stages, while attracting seed and fruit dispersers when the fruits were mature and ripe.

The proximate mechanisms leading to the temporal and spatial dynamics of CPT and related compounds during fruit development are however, not yet clearly understood. Recovery of two intermediates of CPT biosynthesis, namely, strictosamide and deoxypumiloside in the seed tissues suggests a *de novo* synthesis of CPT in the seed, besides the possibility of transport of CPT into the seeds. The reduction in CPT content upon ripening could arise both due to the degradation and or remobilization of CPT into other plant parts. Mass spectrometric analysis of the ripened fruits did not reveal any mass signatures of degradative products.

1. Hsiang, Y. H., Hertzberg, R., Hecht, S. and Liu, L. F., Camptothecin induces protein-linked DNA breaks via mammalian DNA topoisomerase I. *J. Biol. Chem*., 1985, **260**, 14873–14878.
2. Thomas, C. J., Rahier, N. J. and Hecht, S. M., Camptothecin: current perspectives. *Bioorg. Med. Chem*., 2004, **12**, 1585–1604.
3. Pantazis, P., Han, Z., Chatterjee, D. and Wyche, J., Water-insoluble camptothecin analogues as potential antiviral drugs. *J. Biomed. Sci*., 1999, **6**, 1–7.
4. Sadaie, M. R., Mayner, R. and Doniger, J., A novel approach to develop anti-HIV drugs: adapting non-nucleoside anticancer chemotherapeutics. *Antiviral Res*., 2004, **61**, 1–18.
5. Bodley, A. L. and Shapiro, T. A., Molecular and cytotoxic effects of camptothecin, a topoisomerase I inhibitor, on trypanosomes and *Leishmania*. *Proc. Natl. Acad. Sci. USA*, 1995, **92**, 3726–3730.
6. Ramesha, B. T. *et al.*, New plant sources of the anti-cancer alkaloid, camptothecine from the Icacinaceae taxa, India. *Phytomedicine*, 2013, **20**, 521–527.
7. Suma, H. K., Kumar, V., Senthilkumar, U., Kumara, P. M., Ravikanth, G., Santhoshkumar, T. R. and Shaanker, R. U., *Pyrenacantha volubilis* Wight. (Icacinaceae), a rich source of camptothecine and its derivatives from the Coromandel Coast forests of India. *Fitoterapia*, 2014, **97**, 105–110.
8. Hemalatha, R. G. and Pradeep, T., Understanding the molecular signatures in leaves and flowers by desorption electrospray ionization mass spectrometry (DESI MS) imaging. *J. Agricul. Food. Chem*., 2013, **61**, 7477–7487.
9. Ifa, D. R., Srimany, A., Eberlin, L. S., Naik, H. R., Bhat, V., Cooks, R. G. and Pradeep, T., Tissue imprint imaging by desorption electrospray ionization mass spectrometry. *Anal. Methods*, 2011, **3**, 1910–1912.
10. Mohana Kumara, P., Srimany, A., Ravikanth, G., Uma Shaanker, R. and Pradeep, Y., Ambient ionization mass spectrometry imaging of rohitukine, a chromone anti-cancer alkaloid, during seed development in *Dysoxylum binectariferum* Hook.f (Meliaceae). *Phytochemistry*, 2015, **116**, 104–110.
11. Li, B., Bjarnholt, N., Hansen, S. H. and Janfelt, C., Characterization of barley leaf tissue using direct and indirect desorption electrospray ionization imaging mass spectrometry. *J. Mass Spectrom*., 2011, **46**, 1241–1246.
12. Thunig, J., Hansen, S. H. and Janfelt, C., Analysis of secondary plant metabolites by indirect desorption electrospray ionization imaging mass spectrometry. *Anal. Chem.*, 2011, **83**, 3256–3259.
13. Yan, X. F., Wang, Y., Yu, T., Zhang, Y. H. and Dai, S. J., Variation in camptothecin content in *Camptotheca acuminata* leaves. *Bot. Bull. Acad. Sin*., 2003, **44**, 99–105.
14. Cabral, E., Mirabelli, M., Perez, C. and Ifa, D., Blotting assisted by heating and solvent extraction for DESI-MS imaging. *J. Am. Soc. Mass Spectrom*., 2013, **24**, 956–965.
15. Srimany, A., Ifa, D. R., Naik, H. R., Bhat, V., Cooks, R. G. and Pradeep, T., Direct analysis of camptothecin from *Nothapodytes nimmoniana* by desorption electrospray ionization mass spectrometry (DESI-MS). *Analyst*, 2011, **136**, 3066–3068.
16. Borisjuk, L., Walenta, S., Rolletschek, H., Mueller-Klieser, W., Wobus, U. and Weber, H., Spatial analysis of plant metabolism: sucrose imaging within *Vicia faba* cotyledons reveals specific developmental patterns. *Plant J*., 2002, **29**, 521–530.
17. Alves, M., Sartoratto, A. and Trigo, J. R., Scopolamine in *Brugmansia suaveolens* (Solanaceae): defense, allocation, costs and induced response. *J. Chem. Ecol*., 2007, **33**, 297–309.
18. Fang, J., Reichelt, M., Hidalgo, W., Agnolet, S. and Schneider, B., Tissue-specific distribution of secondary metabolites in rapeseed (*Brassica napus* L.). *PLoS. ONE*, 2012, **7**, e48006.
19. Telek, L., Delpin, H. and Cabanillas, E., *Solanum mammosum* as a source of solasodine in the lowland tropics. *Econ. Bot*., 1977, **31**, 120–128.
20. Sharma, N. S., Varghese, S., Desai, J. and Chinoy, J. J., Biosynthesis of solasodine in developing berries of *Solanum khasianum* Clarke. *Indian. J. Exp. Biol.*, 1979, **17**, 224–255.
21. Kozukue, N. and Friedman, M., Tomatine, chlorophyll, *β*-carotene and lycopene content in tomatoes during growth and maturation. *J. Sci. Food. Agric*., 2003, **83**, 195–200.
22. Hebbar, R., Sashidhar, V. R., Uma Shaanker, R., Udaya Kumar, M. and Sudharshana, L., Dispersal mode of species influences the trypsin inhibitor levels in fruits. *Naturwissenschaften*, 1993, **80**, 519–521.

ACKNOWLEDGEMENTS. We thank the Department of Biotechnology (No. BT/PR8266/NDB/39/266/2013) and Department of Science and Technology, Government of India for financial support. P.M.K. thanks IIT Madras, for a postdoctoral fellowship and A.S. thanks the Council of Scientific and Industrial Research, Government of India for research fellowship.

Received 12 December 2015; accepted 27 September 2016

doi: 10.18520/cs/v112/i05/1034-1038

A cognitive method for building detection from high-resolution satellite images

Naveen Chandra* and Jayanta Kumar Ghosh

Department of Civil Engineering, Indian Institute of Technology, Roorkee 247 667, India

In recent years, high-resolution satellite (HRS) images have become an important source of data for extracting geo-spatial information. A deep understanding of human cognitive capabilities is required in order to automate the method of information retrieval from HRS images. The aim of this study is to emulate human cognitive processes by integrating cognitive task analysis for information extraction from HRS images. First, the preliminary knowledge about the cognitive processes which human beings acquire during the interpretation of satellite images is collected. Then, knowledge is represented in the form of rules which are based on the visual interpretation of the images by the human beings. During knowledge elicitation these rules are used to extract buildings from HRS images utilizing the mixture tuned matched filtering algorithm. Later, the method is tested using 14 HRS images of an urban area. The average of precision, recall and *F*-score is computed as 79.45%, 64.34% and 70.28% respectively.

Keywords: Building detection, cognitive processes, high-resolution satellite images, urban areas.

*For correspondence. (e-mail: naveenchandra0408@gmail.com)